Adaptive Optics for Vision Science and Astronomy
*ASP Conference Series, Vol. **VOLUME**, **PUBLICATION YEAR***
A. Quirrenbach

Low Cost Adaptive Optics

Chris Dainty, Ian Munro and Carl Paterson

Blackett Laboratory, Imperial College, London SW7 2BW, England

Abstract.
Building a low cost adaptive optics system of moderate performance is not difficult in principle, and in this article one approach adopted by our group is described. Our system is based on a membrane mirror, a Shack-Hartmann sensor and a simple control system. Two breadboard AO systems are described and we speculate on some possible future developments.

1. Introduction

The first working adaptive optical (AO) systems were built by the US military for a cost at which we can only guess, certainly many tens of millions of dollars in today's terms. When adaptive optics was taken up by astronomers, they managed to reduce the cost but still an AO system for a large telescope costs several million dollars. Why? If we can identify and understand why an astronomical AO system is so expensive, we will have the basic knowledge to construct a low cost system. It is very important to appreciate that astronomical AO systems are expensive for clearly identifiable (and justifiable) reasons, and that when building a low cost system for other applications some compromises are necessary.

First we should define "low cost". A CD or DVD read head is an adaptive optical system with tracking and focus control: the whole optical assembly, consisting of laser, optics and detector costs only a few dollars. Clearly, the economies of scale of producing tens of millions of units contributes largely to this very low cost. For higher order AO systems, people are still looking for a high-volume application, and so the approach by ourselves and others has been to produce an inexpensive single instrument, an experimental breadboard which we can use to learn about AO and to demonstrate the possibilities of AO in different applications. The first system we built cost approximately $25K in parts and took approximately three person-years of post-doc labour to construct. The second system cost $20K and took four months of labour from start to finish. We call both of the these systems "low cost".

A key step in the development of low cost AO systems is the development of enabling technologies, particularly, in the case of AO, wavefront sensor detectors and deformable mirrors or other correcting devices. These enabling technologies may require a very large investment: for example, current detectors are typically CCD cameras, or CMOS cameras in the future, and the development of both of these represent enormous investments. Clearly, if AO can capitalise on com-

mercially available components — preferably ones used in consumer products — the cost of AO systems can be dramatically reduced.
Any "one-off" optical system is necessarily expensive, but why are astronomical AO systems so expensive? Some of the reasons are:

1. The wavefront sensor must be extremely efficient, involving low-noise, high-QE, high-speed CCDs. Complete with controller, these CCDs cost \$30K – \$100K. Alternatively, avalanche photodiodes might be used, one for each element of the wavefront sensor (e.g. 19 were used in PUEO (Rigaut et al 1998), and these cost about \$5K each).

2. Astronomical systems frequently have fairly high-order correction, and this involves high-quality, expensive deformable mirrors: these cost \$1000 to \$2000 per actuator, depending upon the bandwidth of the high-voltage amplifiers.

3. Astronomical AO systems have to operate at a moderate bandwidth, up to 1KHz open loop frame rate. This means that custom data-flow and control systems are required, particularly to eliminate any time lag between the wavefront sensor and the transmission of deformable mirror voltages.

4. At an astronomical observatory, the AO system has to be integrated with the types of control architecture already in use, such as EPICS. The software effort required to build a user-friendly system compliant with all the other requirements of the observatory can be very large.

5. Finally, and not to be underestimated, astronomical AO projects are high-profile ventures in which the possibility of failure cannot be accepted. This in turn means that rather conservative, expensive solutions are preferred over inexpensive innovative ones, with large teams of engineers rather than small university groups. Prior to any construction of hardware, a huge modelling and design effort amounting to several \$100Ks, with formal conceptual design reviews, provisional design reviews, etc is carried out. It is worth remarking that there have been exceptions to this general trend: the curvature AO systems developed by Roddier, Northcott and Graves (1991) are the most efficient astronomical AO systems and were built on a relatively small budget by a small university-based team.

In contrast to the above, our first AO system was built without any prior modelling or formal design process, at least on the scale encountered in astronomy. All the components were available commercially, and no attention was paid to photon-efficiency of the wavefront sensor. A 37-element membrane mirror costing \$1000 was used as the deformable mirror. Arrays of digital signal processing chips used in astronomical AO systems were replaced by a single DSP in the first system, and by a single 500MHz Pentium III in the second system. The resultant system has many imperfections but nevertheless it has good performance, particularly regarding bandwidth.

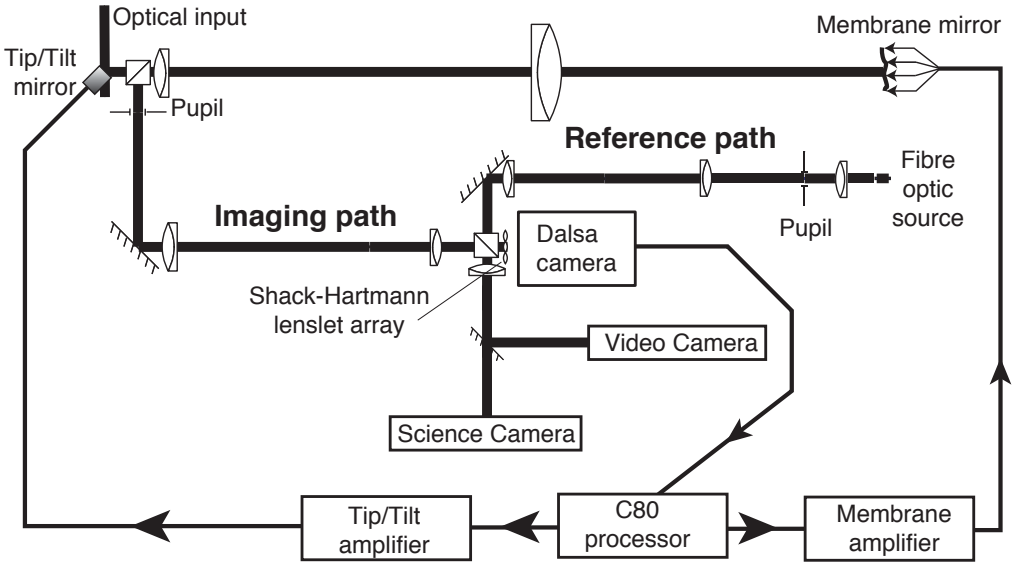

Figure 1. Schematic layout of optical breadboard.

2. Description of System

A detailed description of our first system can be found in Paterson, Munro & Dainty (2000), and here we give only an outline of the essential features. Figure 1 shows a schematic diagram of the layout of the system. The original idea was to build a general purpose system that could be used with various mirrors (or liquid crystal correctors) and wavefront sensors, so the optical breadboard was rather large, $0.6 \times 1.5\,\mathrm{m}$.

The beam enters the system via a tip-tlt mirror (Physik Instrumente Model E610.00): in practice, this may not be necessary when a membrane is used as the main deformable mirror but it can be switched in if necessary. The tip-tilt mirror was the single most expensive item in the breadboard set-up (approximately \$7K). The deformable mirror is a 15mm diameter membrane mirror (OKO Technologies, Delft, http://www.okotech.com/mirrors/technical/index.html) with 37 hexagonal electrodes on a 1.75mm spacing (Vdovin & Sarro 1995) and we have generally used Grade B devices whose flatness is typically on the order of one wave of visible light. A series of low-aperture (large F-number) doublets ensure that the tip-tilt mirror, deformable mirror and wavefront sensor are all conjugate to each other: this involves a de-magnification on the order of ten from the deformable mirror to the wavefront sensor. The Shack-Hartmann wavefront sensor has lenslets on a rectangular pitch of 0.2mm of focal length 25mm and uses an 8-bit Dalsa CCD camera (model CA-D1-0128A) with 128×128 16 μm square pixels. The camera operates at up to 780 frames per second. Unlike an astronomical AO system, we do not currently use quad cells but rather each Shack-Hartmann spot is sensed by a large number of pixels (for example 8×8). Typically, a matrix of 5×5 Shack-Hartmann spots provides adequate sampling for the 37-element membrane mirror.

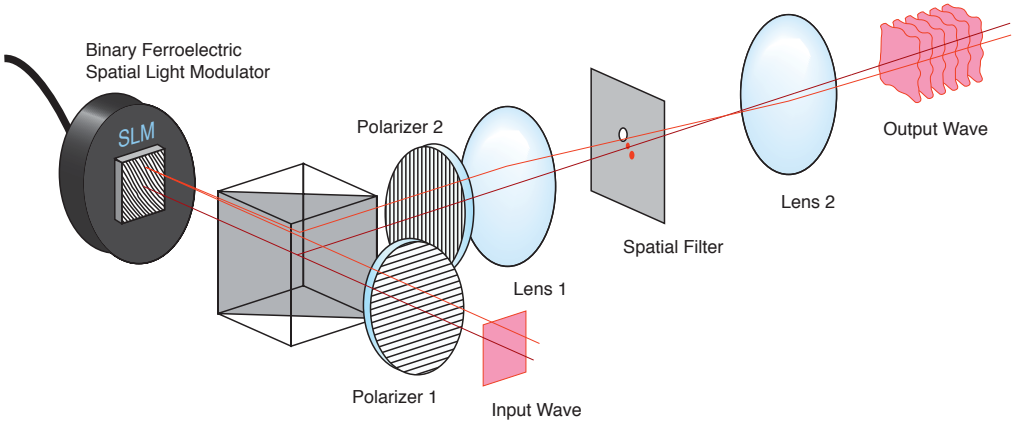

Figure 2. Schematic layout of simulation set-up.

The wavefront sensor needs a plane-wave reference beam for calibration. This is provided by a point source from a single-mode fibre and a large F-number doublet, as shown in Figure 1. In our system, this typically produced a beam with a Strehl ratio on the order of 0.8.

The input test beam to be corrected is generated by dynamic holography using a scheme first suggested by Neil, Booth and Wilson (1998): a sequence of 128 pseudo-Kolmogorov wavefronts are generated in a computer (see Glindemann, Lane & Dainty 1993), encoded as an off-axis phase hologram movie of 128 frames, and transferred to a Displaytech 256 $\times$ 256 pixel ferro-electric liquid crystal spatial light modulator, which is read-out in reflection (see Figure 2) at up to 2.5 KHz frame rate. This enables us to generate wavefronts with pseudo-Kolmogorov statistics[1] or any other time-varying wavefront for test purposes.

The data flow and control system are shown in Figure 3. One of the biggest problems in using commercially available components, particularly frame grabbers, is the delay between the acquisition of a frame and its availability to the control system. We believe there is between a one- and two-frame delay in the system shown in Fig. 3, which uses a Bitflow Roadrunner framegrabber. In our first system, we used a Texas Instruments C80 Digital Signal Processor (DSP) to control the AO system. The two basic tasks are to locate the centroids of the Shack-Hartmann spots and to transform the centroid data (typically 25 x-coordinates and 25 y-coordinates) to electrode (or actuator) voltages for the membrane mirror (typically 37 electrodes). The C80 is linked to a PC via the PCI bus, and originally transmitted the voltages to the membrane mirror via an ISA bus D-to-A card, thus requiring the use of the PC for this task. This is clearly suboptimal and recently a PCI-bus D-to-A converter (SBS Greenspring, IP-FastDAC industry pack modules) has been used and driven directly by the C80.

[1]The test wavefront is cyclic and has limited outer scale, hence the tip and tilt is smaller than for a Kolmogorov wavefront with infinite outer scale.

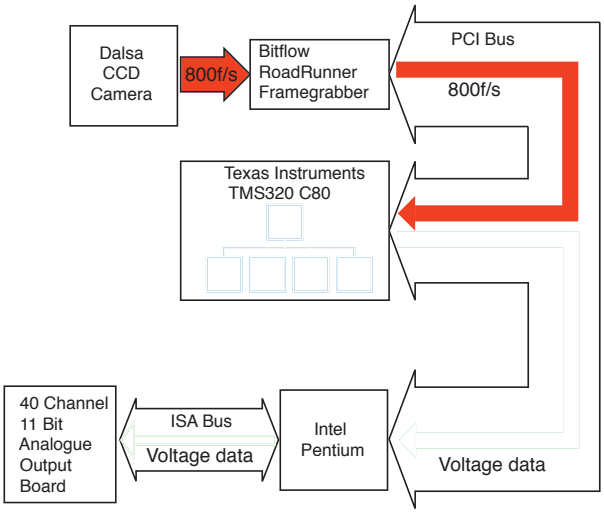

Figure 3. Original data flow and control system. A later update of this system used a PCI D-to-A card with direct control by the C80.

The control system used is an elementary one in which the temporal and spatial parts are treated separately. For the temporal control, a simple integrator is used. Denoting the mirror actuator control[2] vector at the nth iteration by $\mathbf{x}_n$,

$$\mathbf{x}_n = (1 - \beta)\mathbf{x}_{n-1} + g\mathbf{M}\mathbf{s}_n \tag{1}$$

where g is the integrator gain, $\mathbf{M}$ is the spatial control matrix, $\mathbf{s}$ is the sensor signal vector (x- and y-coordinates of Shack-Hartmann spots) and $\beta \ll 1$ is a bleed parameter to make the system resistant to possible modes of the mirror that are invisible to the wavefront sensor. Suitable values of β and g were chosen by trial-and-error.
The spatial control matrix is found as follows. Assuming linearity, the sensor signal vector $\mathbf{s}$ is related to the actuator control vector $\mathbf{x}$ by a matrix $\mathbf{A}$:

$$\mathbf{s} = \mathbf{A}\mathbf{x}. \tag{2}$$

The matrix $\mathbf{A}$ is called the system matrix: it is found by successively applying the same fixed control signal value to each actuator in turn (with zero control signal applied to all other actuators[3]) and recording the sensor vector, thus building up the matrix column by column. We refer to this as the calibration stage, and since this only takes a second or two in our system, we calibrate the

[2]It should be noted that the mirror deformation is not linear with voltage

[3]In fact, because the membrane mirror can only be deformed in one direction, we have to apply a bias to allow correction in both directions. This means that actuator controls set to zero do not correspond to zero voltage on the device itself.

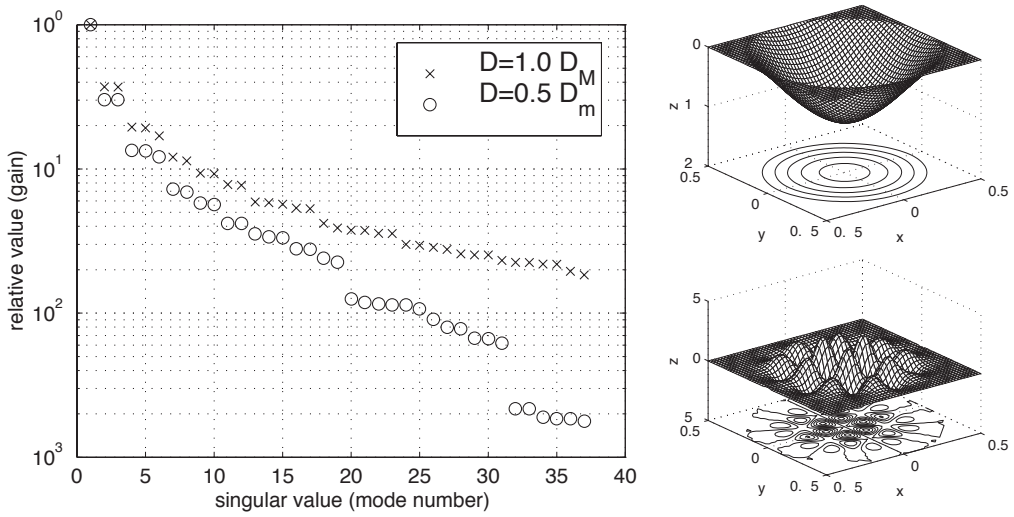

Figure 4. Left: Relative magnitude of the singular values as a function of the mode number. Right: the 1st (upper) and 37th (lower) mirror deformation modes.

system frequently to avoid any unknown instabilities. The system matrix **A** can be decomposed by singular value decomposition:

$$\mathbf{A} = \mathbf{USV}^T \tag{3}$$

where the columns **U** and **V** are the sensor signal and actuator control modes of the system, and **S** is a diagonal matrix of singular values, one for each mode. An understanding of the behaviour of the singular values is important for stable and effective operation of the control system. The right hand side of Figure 4 shows the first and thirty-seventh modes that result from a singular value decomposition of the influence matrix of the mirror (this is the equivalent of the matrix **A** but relating mirror control vectors to mirror deformations). The left hand side plots the singular values as a function of the mode number. The singular values represent the gains of the system: a small singular value means that a large actuator voltage is required to produce unit amplitude of a given deformation mode. The ratio of the largest singular value to the smallest is the condition factor and is a measure of the controllability of the mirror.
The control matrix **M** (see Eq. 1) is the pseudo-inverse of the matrix **A**:

$$\mathbf{M} = \mathbf{A}^{-1} = \mathbf{VS}^{-1}\mathbf{U}^T \tag{4}$$

Clearly, modes with small singular values will have a large effect on the actuator voltages leading to clipping of the signals: as will be seen, discarding these modes improves the performance of the system.

3. Results

We have typically used a membrane mirror whose flatness (with the actuator controls set to zero) was on the order of one visible wavelength. Thus the image

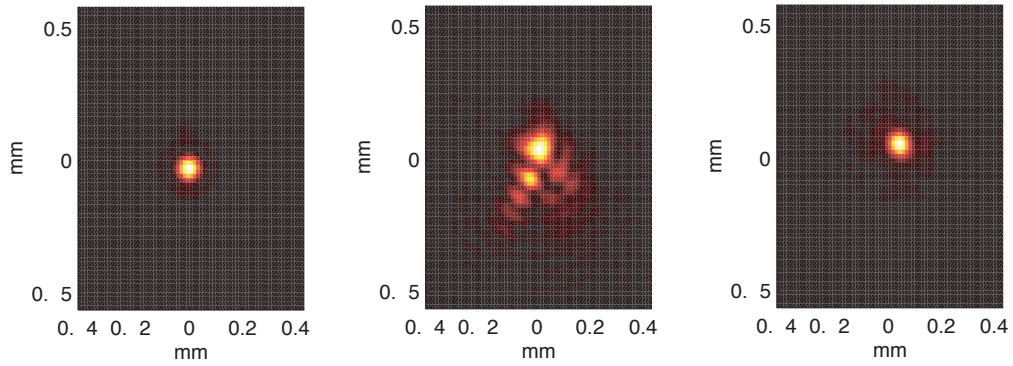

Figure 5. Left: Point spread function of reference beam. The Strehl ratio is ≈0.82. Centre: Point spread function with membrane mirror in the system but with zero control signal applied to the actuators. Right: Point spread function with static errors corrected. The Strehl ratio is ≈0.74.

quality with the actuator controls set to zero is rather low. Figure 5 (left) shows the reference image, with a measured Strehl ratio[4] of approximately 0.82. The centre image shows the point spread function of the system with no control signal applied to the membrane mirror, showing coma introduced by the relatively poor mirror flatness. The right hand side of Fig. 5 shows the static corrected image, with a Strehl of 0.74: this is the best point spread function obtainable with the system.

To illustrate dynamic correction, the turbulence generator is set to simulate a single layer of turbulence moving (without evolution, in accordance with the Taylor hypothesis) at velocity v: in this case, a complete new sample of turbulence is presented to each Shack-Hartmann lenslet ($\approx r_0$) in a time v/r_0. In the following, pseudo-Kolmogorov turbulence is generated with a value of D/r_0 of approximately 7.5. Figure 6 shows the degree of correction achieved in the case in which $v/r_0 \approx 5$Hz: a movie of this can be viewed in Paterson et al (2000). In this case, approximately 25 modes were used in the control loop. Figure 7 shows the effect on the Strehl ratio of using different numbers of modes (the higher reciprocal singular values in Eq. 3 are simply set to zero for the modes to be discarded): using all 37 modes is worse than using only one, and the optimum number lies between 20 and 25. Finally, Figure 8 shows the Strehl ratio as a function of the parameter v/r_0 for our system operating at 780fps and $D/r_0 \approx 5$. A value of $v/r_0 = 100$Hz — where our system still produces a decent Strehl ratio — corresponds to a wind speed of 50ms^{-1} (>100mph) for a value of $r_0 = 0.5$m, indicating that our system has sufficient bandwidth for infrared astronomy.

[4]The Strehl ratio was measured by comparison of the image of a point source with that expected assuming a diffraction limited system of the same aperture: this procedure in our case has an uncertainty on the order of 5%.

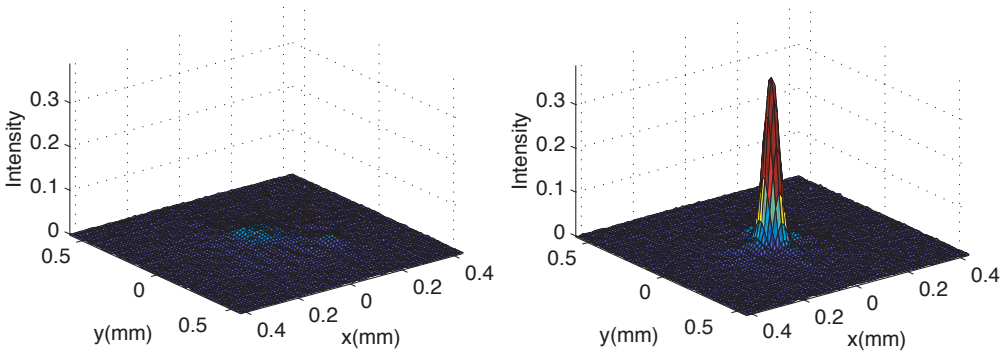

Figure 6. Time-averaged point spread functions without (left) and with (right) the AO system in operation, for pseudo-Kolmogorov turbulence with $D/r_0 \approx 7.5$. For this figure, the frame rate was 270 fps and $v/r_0 \approx 5$.

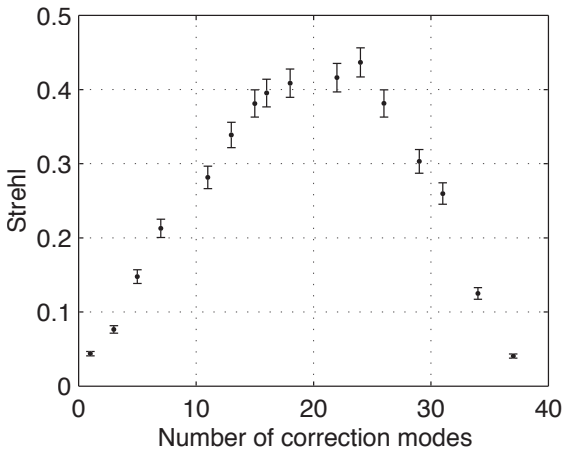

Figure 7. Strehl ratio as a function of the number of spatial modes used in the control loop, for the system of Fig. 6.

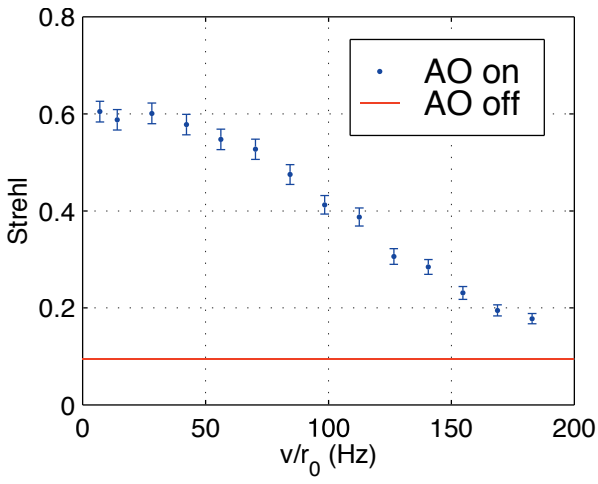

Figure 8. Strehl ratio as a function of the parameter v/r_0, for 780 fps frame rate and $D/r_0 \approx 5$.

4. Second Breadboard System

Our second system is very similar to the first one described above, with the following principal differences:

1. The whole system, including the turbulence generator, is contained on a 600 × 600mm breadboard. It is transportable and has been demonstrated at three locations in addition to our laboratory.

2. The Bitflow Roadrunner framegrabber has been replaced by a Mutech framegrabber (model MV1500) with a Linux driver.

3. Instead of the C80 DSP, we use a single 500 MHz Pentium III, programmed in C++ and running under the Linux operating system. Using this system, the determination of the centroids of the 5 × 5 Shack-Hartman spot and the matrix inversion takes approximately 200μs, and thus the 780 fps frame rate of the Dalsa CCD limits the speed of the system (together with the delay of the framegrabber).

The performance of this second system is essentially the same as that of the first. We have shown in this second system that a special control processor is not required, and that a single general-purpose processor, such as a Pentium, can be successfully used. In our configuration, which uses a 780 fps Dalsa CCD, we believe we could easily cope with a 7 × 7 or 8 × 8 Shack-Hartmann and a 55-actuator mirror[5].

[5] A 55-actuator, 25mm diameter membrane mirror is available from OKO Technologies.

5. Conclusions and Future Work

The aim of our work was to learn how to build adaptive optics systems, and to remove some of the mystique that surrounds the construction of very expensive astronomical AO systems. We have shown that high-performance AO systems can be built at relatively low cost. The availability of inexpensive corrective elements is clearly critical, and several other technologies, in addition to membrane mirrors, are feasible such as bimorph mirrors[6] (Kudryashov and Shmalhausen 1996), liquid crystal correctors (Kelly and Love 1999) and MEMS mirrors (Bifano et al 1999).
There are of course many improvements that could be made to our systems. Some of these are:

1. The combination of a Shack-Hartmann slope sensor with a curvature-based membrane mirror is fundamentally weak. Ideally, one would use some type of curvature sensor, such as the one originally proposed by Roddier (1988) or the novel device of Paterson and Dainty (2000).

2. The use of commercial framegrabbers has caused us a problem, as they introduce an unknown amount of delay into the control loop. It is possible that framegrabbers with zero or minimum delay exist. Another constraint is that we had to choose framegrabbers with suitable drivers provided (a Linux driver was required for the second system and this limited the choice).

3. The Dalsa camera performs well but it is rather expensive (≈$5K including power supply). If one can tolerate the slower speed of conventional video-rate cameras, there are a number of much lower cost solutions. One system currently under construction in our laboratory uses an inexpensive CMOS detector.

4. We have only used the simplest control algorithm and there is considerable scope for improvement in this area.

Future developments are likely to be linked closely with specific applications of adaptive optics. For example, for applications in ophthalmology where video-rate (25–30Hz) frame rate is believed to be sufficient, we envisage that Pentium-based control will easily cope with spatial complexity on the order of 100 actuators.
Two applications-independent developments are envisaged:

1. There are likely to be further developments towards miniaturisation and integration of the optical sub-systems, such as compact modules which house both the wavefront sensor and deformable mirrors in a single unit.

2. In embedded systems, one would wish to eliminate the need for a standard personal computer with its associated peripherals. There is a need to develop compact integrated control systems that do not require a PC, and

[6] We have demonstrated one of our systems working with a 14 element bimorph mirror.

that also eliminate the data delay problem of framegrabbers. In principle these could be very low cost systems (<$500).

6. Acknowledgements

Our adaptive optics programme is supported by grants from the UK Engineering and Physical Sciences Research Council (GR/M 46846 and GR/R04928/01) and the ESPRIT Programme of the European Community (MOSIS: 31063).

References

Bifano, T.G., Perreault, J., Mali, R.K., and Horenstein, M.N. 1999, IEEE J. Sel. Top. Quant. Electron., 5, 83.

Glindemann, A., Lane R.G., & Dainty J.C. 1993, J. Mod. Opt., 40, 2381.

Kelly, T.L., and Love, G.D. 1999, Appl. Opt., 38, 1986.

Kudryashov, A.V., and Shmalhausen, V.I. 1996, Opt. Engng., 35, 3064.

Neil, M.A.A., Booth M.J., & Wilson, T., 1998, Opt. Lett., 23, 1849.

Paterson, C., Munro, I., & Dainty, J.C. 2000, Opt. Expr., 6, 175 (http://www.opticsexpress.org/oearchive/source/20597.htm).

Paterson, C., & Dainty, J.C. 2000, Opt. Lett., 25, 1687.

Restaino S, Dayton D, Browne S., Gonglewski, J., Baker, J., Rogers, S., McDermott S., Gallegos J., & Shilko M., 2000, Opt. Expr., 6, 2.

Rigaut, F., Salmon, D., Arsenault, R., Thomas, J., Lai, O., Rouan, D., Véran, J.P., Gigan, P., Crampton, D., Fletcher, J.M., Stilburn, J., Boyer, C., and Jagoural, P. 1998, Publ. Astr. Soc. Pac., 110, 152.

Roddier, F. 1988, Appl. Opt. 27, 1223.

Roddier, F., Northcott, M., and Graves, J.E. 1991, Publ. Astr. Soc. Pac., 103, 131.

Vdovin, G. & Sarro, P.M. 1995 Appl. Opt., 34, 2695.